

Creation and annihilation phenomena of electron and positron pairs in an oscillating field

M Jiang(江淼), D D Su(苏丹丹), N S Lin(林南省), and Y J Li(李英骏)

Citation: Chin. Phys. B, 2021, 30 (**7**): 070306. DOI: 10.1088/1674-1056/abe378
Journal homepage: http://cpb.iphy.ac.cn; http://iopscience.iop.org/cpb

What follows is a list of articles you may be interested in

Approximate analytical solutions and mean energies of stationary Schrödinger equation for general molecular potential

Eyube E S, Rawen B O, and Ibrahim N
Chin. Phys. B, 2021, 30 (**7**): 070301. DOI: 10.1088/1674-1056/abe371

Wave-particle duality relation with a quantum *N*-path beamsplitter

Dong-Yang Wang(王冬阳), Jun-Jie Wu(吴俊杰), Yi-Zhi Wang(王易之), Yong Liu(刘雍), An-Qi Huang(黄安琪), Chun-Lin Yu(于春霖), and Xue-Jun Yang(杨学军)
Chin. Phys. B, 2021, 30 (**5**): 050302. DOI: 10.1088/1674-1056/abeb0f

Effects of postselected von Neumann measurement on the properties of single-mode radiation fields

Yusuf Turek(玉素甫·吐拉克)
Chin. Phys. B, 2020, 29 (**9**): 090302. DOI: 10.1088/1674-1056/ab9f23

Dynamical effects of switching a super-critical well potential on pair creation from a vacuum

Qiang Wang(王强), Qin-Zhi Xia(夏勤智), Jie Liu(刘杰), Li-Bin Fu(傅立斌)
Chin. Phys. B, 2018, 27 (**8**): 080302. DOI: 10.1088/1674-1056/27/8/080302

Enhanced electron–positron pair creation by the frequency chirped laser pulse

Jiang Min, Xie Bai-Song, Sang Hai-Bo, Li Zi-Liang
Chin. Phys. B, 2013, 22 (**10**): 100307. DOI: 10.1088/1674-1056/22/10/100307

Creation and annihilation phenomena of electron and positron pairs in an oscillating field*

M Jiang(江淼)[1,2], D D Su(苏丹丹)[3], N S Lin(林南省)[1,2], and Y J Li(李英骏)[1,2,†]

[1] School of Science, China University of Mining and Technology, Beijing 100083, China
[2] State Key Laboratory for Geomechanics and Deep Underground Engineering, China University of Mining and Technology, Beijing 100083, China
[3] Beijing National Laboratory for Condensed Matter Physics, Institute of Physics, Chinese Academy of Sciences, Beijing 100190, China

(Received 26 November 2020; revised manuscript received 24 January 2021; accepted manuscript online 5 February 2021)

The combination of an oscillating and a static field is used to study the creation and annihilation phenomena during the pair creation process. The time evolution, spatial density and momentum distribution of the created particles for a fermionic system are presented, which demonstrate that with the increasing static field intensity, the number of the created particles experiences a distinguishable decrease in every period of the oscillating field, which is caused by the annihilation phenomena between the created electrons and positrons.

Keywords: pair creation, computational quantum field theory, strong laser field

PACS: 03.65.–w, 42.25.Bs, 03.65.Pm, 12.20.Ds **DOI:** 10.1088/1674-1056/abe378

1. Introduction

One of the most fascinating subjects in high energy physics is that the vacuum can be polarized under an external strong field, which is predicted by the theory of quantum electrodynamics. In 1951, Schwinger calculated the threshold of the "breakdown" vacuum under an ultra-strong static electric field,[1] which attracts a number of experts to study pairs creation under different external fields.[2–12] The critical value of the vacuum polarization for a time-independent and spatially homogeneous electric field is $E_c = 1.32 \times 10^{16}$ V/cm, which requires a laser beam with the tremendous intensity about 10^{29} W/cm^2. Under the present experimental condition, it cannot be achieved to observe the particle pairs creation phenomenon directly from the vacuum only due to the effect of light. However, recent research has come into view using the extremely high-power laser field due to the continued advancement of the laser-based system. With the rapid development of the laser technique, it is believed that in the near future, the intensity of the laser will be able to approach or even reach the Schwinger limitation.

The particle pairs can be created from vacuum due to three mechanisms. The first mechanism is called the Schwinger tunnelling effect.[13–15] It requires a static electric field that exceeds $E_c = 1.32 \times 10^{16}$ V/cm and the particle-pairs can be created persistently from the vacuum under this ultra-strong external electric field. The second mechanism indicates that the electron-positron pairs can also be created permanently when the external electric field changes rapidly over time, which is known as the photon transition effect.[16–18] For the third mechanism, to generate particle pairs, the supercritical quasi-bound state caused by a supercritical potential well is required.[19–24] To further understand the pair creation process, more sophisticated field configurations are applied, which requires the combination of the above fields. Some studies combined a static strong field with an oscillating field, such a combination will induce the dynamically assisted Schwinger effect, which has been wildly discussed recently.[16,25–27]

2. Quantum field theoretical simulations

In order to describe the pair creation process, in this paper we apply the numerical solution of the Dirac equation on whole time and space scale by applying the quantum field theory.[28,29] We consider a one-dimensional system, in which the evolution of the field operator $\hat{\Psi}(z,t)$ can be expanded in terms of creation and annihilation operators and positive and negative energy states

$$\begin{aligned}\hat{\Psi}(z,t) &= \sum_p \hat{b}_p(t)u_p(z) + \sum_n \hat{d}_n^{\dagger}(t)v_n(z) \\ &= \sum_p \hat{b}_p u_p(z,t) + \sum_n \hat{d}_n^{\dagger} v_n(z,t). \end{aligned} \tag{1}$$

The subscripts p and n in this equation represent positive and negative energy, respectively. Here $u_p(z)$ and $v_n(z)$ are the initial positive and negative states that can be obtained by solving the force-free Dirac equation, while $\hat{b}_p$ and $\hat{d}_n^{\dagger}$ denote the annihilation and creation operators for positive or negative state, respectively.

To obtain the spatial density and total number of created electrons, the electronic portion of the field operator associated

*Project supported by the National Natural Science Foundation of China (Grant Nos. 11974419 and 11605286), the Strategic Priority Research Program of Chinese Academy of Sciences (Grant No. XDA25051000), and the National Key R&D Program of China (Grant No. 2018YFA0404802).

†Corresponding author. E-mail: lyj@aphy.iphy.ac.cn

© 2021 Chinese Physical Society and IOP Publishing Ltd

with positive energy can be defined as

$$\hat{\Psi}^{(p)}(z,t) = \sum_p \hat{b}_p(t) u_p(z). \tag{2}$$

The spatial density of created electron is defined as

$$\rho(z,t) = \langle\langle \text{vac}||\hat{\Psi}^{\dagger(p)}(z,t)\hat{\Psi}^{(p)}(z,t)||\text{vac}\rangle\rangle, \tag{3}$$

where $||\text{vac}\rangle\rangle$ denotes the vacuum state. Using the two equivalent expressions for the time evolution of the field operator $\hat{\Psi}(z,t)$ in Eq. (1) and the initial state property $\hat{b}_p||\text{vac}\rangle\rangle = 0$, after some algebra the spatial density can be obtained as follows:

$$\rho(z,t) = \sum_p \sum_n |\langle u_p(z)|\phi_n(z,t)\rangle|^2. \tag{4}$$

The total number of the created particles can be obtained by integrating $\rho(z,t)$ over space. In Eq. (4), $\phi_n(z,t)$ is the state function for negative states. The evolution of the state function follows the Dirac equation (in atomic units hereafter)

$$\mathrm{i}\frac{\partial}{\partial t}\phi(z,t) = \left[c\alpha_z \hat{p}_z + \beta c^2 + V(z,t)\right]\phi(z,t). \tag{5}$$

Here c is the speed of light in vacuum ($c = 137.036$ a.u.), α_z denotes the z component of the Dirac matrix, and β is the diagonal Dirac matrix. The time-dependent scalar potential associated with the external force acting along the z direction is presented by $V(z,t)$.

The Dirac equation can be solved numerically using the split-operator method,[30,31] while the time evolution operator $\mathrm{e}^{-\mathrm{i}ht}$ is decomposed into multiple consecutive actions, each subinterval operators can be approximated by $\mathrm{e}^{-\mathrm{i}h\Delta t} \simeq \mathrm{e}^{-\mathrm{i}V\Delta t/2} \times \mathrm{e}^{-\mathrm{i}h_0\Delta t} \times \mathrm{e}^{-\mathrm{i}V\Delta t/2}$, while h_0 is the force-free Hamiltonian and the error is of order $O(\Delta t^3)$. Using the Fourier transformation between the spatial and momentum representation, we can compute the action of the corresponding propagators.

3. The creation and annihilation phenomena of particles

In this paper, the one-dimensional model is considered under a combination of scalar potential $V(z) = V_1 S(z)\sin(\omega t) + V_2 S(z)$, which consists of an oscillating electric field and a static electric field, while $S(z) = \{1 + \tanh[(z-z_0)/W]\}/2$ is the Sauter potential.[32] The center of the field is located at z_0 with a width of W. The intensity of the oscillating electric field and static electric field are V_1 and V_2, respectively, while the frequency of the oscillating field is ω.

In this model, the oscillating field and the static field plays different parts during the pair creation process. The oscillating field with a high frequency will create particles continuously, while the created particles will occupy the energy states and block further particle creation due to the Pauli Blocking effect for a fermionic system. The static field is added to clean out the interaction region thus increase the number of created particles. The previous result shows that, while only the oscillating field is applied, both the momentum and the spatial density distribution of the created particles are symmetrical.[25] With the additional static field, the symmetric distribution would be broken and the created particles can be dragged out of the interaction region. However, with a symmetrical distribution, while half of the created particles are accelerated and moving out of the interaction region, the other half would be decelerated and dragged back into the interaction area, thus affect the creation process afterwards.

To analyze these effects, we first obtain the time evolution of the total number of created particles. In Fig. 1, the intensity of the oscillating field is set as $V_1 = c^2$ and the frequency is $\omega = 2.5c^2$, which gives a time cycle $t_\mathrm{e} = 2\pi/\omega = 1.34\times10^{-4}$. Due to the photon transition effect, for a frequency that is larger than the energy gap $2c^2$, particles can be created continuously. Though the total simulation time $t = 0.002$, to focus on the effect of the dragged-back particles, we present the time evolution of the created number from $t = 0.0015$ to 0.002, which gives a better expression of the details. Here we choose four different intensities of the external static field $V_2 = 0$, $0.2c^2$, $0.5c^2$, $0.8c^2$, which are shown in Figs. 1(a), 1(b), 1(c), and 1(d), respectively. We can see that with different intensities of the external static fields, the number of created particles all grows linearly over time, with minor oscillations alone the curves that shape repetitively for each cycle t_e, which is marked with dashed lines in Fig. 1. However, with increasing the intensity of the static field, the curves for each cycle shape differently.

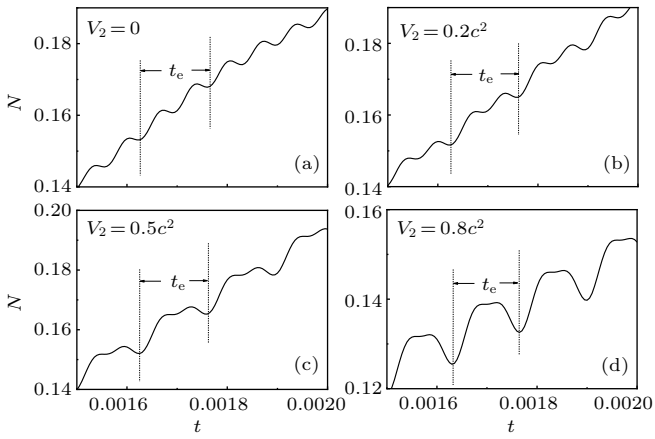


Fig. 1. Time evolution of the total number of created particles under different intensities of the external static field. The amplitude and frequency of the external oscillation field are $V_1 = c^2$ and $\omega = 2.5c^2$, the width of both fields is $W = 3/c$.

In the absence of the static field for $V_2 = 0$ as shown in Fig. 1(a), the oscillating period in time corresponds to $t_\mathrm{e}/2$,

and the time evolutions of the created number in the first half cycle and the second half cycle are identical. This is due to the fact that, if we only apply the oscillating field, the energy of the single-photon will be sufficient to cross the energy gap, then the potential function of the first half period and the last half period will be equivalent. For $V_2 = 0.2c^2$ in Fig. 1(b), such a symmetry would be broken by the static field so the shape of the minor oscillation is slightly different from that for $V_2 = 0$ because the intensity of the static field is relatively small. For $V_2 = 0.5c^2$ in Fig. 1(c), the shapes of the first half cycle and the second half cycle are obviously different, while in the beginning stage of the first half cycle the increase of the created number is more obvious, and in the last stage of the second half cycle the created number decreases faster. In Fig. 1(d) for a intensity $V_2 = 0.8c^2$, both the increase in the first half cycle and the decrease in the second half cycle become steeper, as observed from the curve.

For each period, with different V_2, the creation process behaves differently. For the first half cycle $2n \times t_e/2 < t < (2n+1) \times t_e/2$, the slope of the curves is always positive regardless of the intensity of the static field V_2, and increase faster for stronger field intensity. However, with the increase of the intensity for the static field, in the second half cycle $(2n+1) \times t_e/2 < t < (2n+2) \times t_e/2$ the slopes of the curves gradual reduces and even changes from positive to negative. The slope of curves can be considered as the creation rate of the particles. For a positive creation rate, the system is experiencing a creation phenomenon, while for a negative creation rate, it is considered as an annihilation phenomenon.

The reason is that the created particles (here only consider one kind of particles such as electron or positron) are able to escape from the interaction region to both the left and right directions with the absence of the external static field V_2 (as shown in Fig. 2(a)). However, by adding the external static field (the direction can be assumed as pointing to the left), the left-moving positrons would be accelerated and pushed out of the field region while the right-moving particles are decelerated. For the left-moving accelerated positrons in Fig. 2(b), a stronger static field will evacuate more particles thus increase the total number as shown in the first half cycle in Fig. 1, due to the Pauli blocking principle for a fermionic system. On the other hand, while the static field is strong enough, the right-decelerated-moving particles will be dragged back to the interaction region as presented by Fig. 2(c), and annihilate with the created electrons. Thus, an annihilation phenomenon will appear on the curve as a negative slope, as observed in the second half cycle in Fig. 1. Otherwise, it would be a creation phenomenon if the decelerated particles can not be dragged back to interaction region and keep moving to the right while the static field is relatively weak.

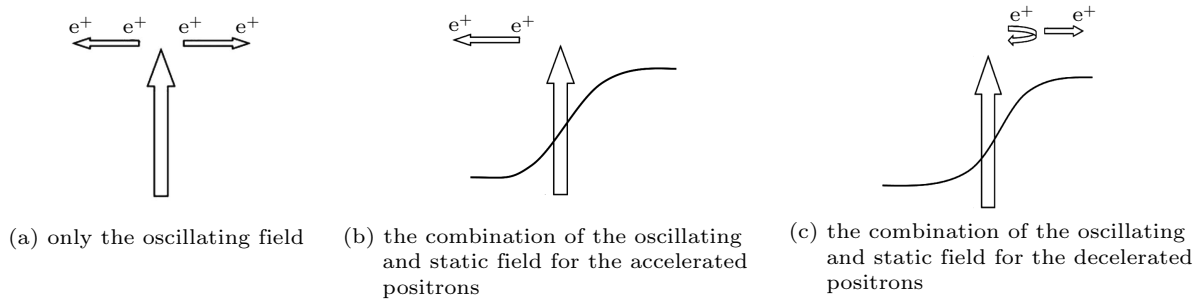


Fig. 2. The different motion modes for the created positrons. (a) Only the oscillating field is applied, which is indicated by an up arrow, and e^+ are the created positrons which head to two directions in one-dimensional simulation. (b) and (c) The created positrons experience three motion modes by adding the static electric potential, which is presented by the solid curve.

The available critical value of the static field is based on the theoretical analysis of the model. The creation mechanism is single-photon transition effect in this situation and the effect of the static field is considered to accelerate or decelerate the created particles. The most probable value of the kinetic energy of the created particle is considered as $\omega - 2c^2$, while ω is the frequency of a single-photon and meanwhile the total energy of a created particle, and $2c^2$ is the rest energy. In this case, the initial velocities of these particles can be obtained as $c\sqrt{1-4c^4/\omega^2}$. For a oscillating field with frequency $\omega = 2.5c^2$ as we choose in Fig. 1, a static field with intensity $V_2 \geq 0.5c^2$ would be able to cancel out the kinetic energy of the created particles thus drag them back into the interaction region and cause annihilation. According to Fig. 1, it is obvious that the annihilation phenomenon appears on the curve in the second half cycle $(2n+1) \times t_e/2 < t < (2n+2) \times t_e/2$ when the external static field intensity $V_2 \geq 0.5c^2$; while the slope is positive when the external static field intensity $V_2 < 0.5c^2$.

We should point out that the initial velocity $c\sqrt{1-4c^4/\omega^2}$ is the most probable velocity of the created particles, while some of the created particles have velocities less or larger than $c\sqrt{1-4c^4/\omega^2}$. As shown in Fig. 1, while the intensity of the static field $V_2 = 0.2c^2$ (in Fig. 1(b)), the curve of the second half cycle is slightly different and the slope is decreased in comparison with Fig. 1(a) in the absence of the static field. For a stronger intensity $V_2 = 0.8c^2$ as shown in Fig. 1(d), more particles are dragged back and the slope becomes even smaller than that for $V_2 = 0.5c^2$ in Fig. 1(c),

which indicates a stronger annihilation effect. On the other hand, for a fermionic system these particles will occupy the quantum states and block the creation of new particles. Besides the annihilation between the particles and antiparticles, the dragged back particles will be eliminated due to the Pauli exclusion principle before they move back to the interaction region.

To analyze the effect of different field width on the creation rate, we define the equivalent creation rate as $\eta = \Gamma/W$, while Γ is the creation rate of the particles and W is the width of the oscillating field. For a smaller field width W, a narrower range of the energy distribution for the created particles can be obtained. Therefore, the energy of the created particles will be more concentrated on the most probable energy $\omega - 2c^2$,[33] and more created particles will be dragged back when the intensity of the external static field exceeds the critical value $V_2 = 0.5c^2$. Figure 3 presents the time evolutions of the created particles for different field widths with the same oscillation intensity and frequency, compared to Fig. 1, when the static field intensity $V_2 = 0.8c^2$. As shown in Fig. 3, the slopes of the curves in the second half cycle $(2n+1) \times t_e/2 < t < (2n+2) \times t_e/2$ decrease with the increase of the field width W. The slopes indicate the creation rates of different field widths $W = 2/c$, $W = 3/c$, $W = 4/c$ and $W = 5/c$, which are $\Gamma_a = -158.9$, $\Gamma_b = -109.8$, $\Gamma_c = -146.3$ and $\Gamma_d = -34.0$, respectively. The equivalent creation rates of these widths are $\eta_a = -79.45$, $\eta_b = -36,6$, $\eta_c = -11.6$ and $\eta_d = -6.8$. For small field width W, more particles with concentrated energy will be dragged back and cause the annihilation phenomenon, thus the negative slope will be steeper. With the increase of the field width, the energy distribution of the created particles becomes wider and less particles will be dragged back, the annihilation effect will be weaker and the absolute value of the negative slope decreases.

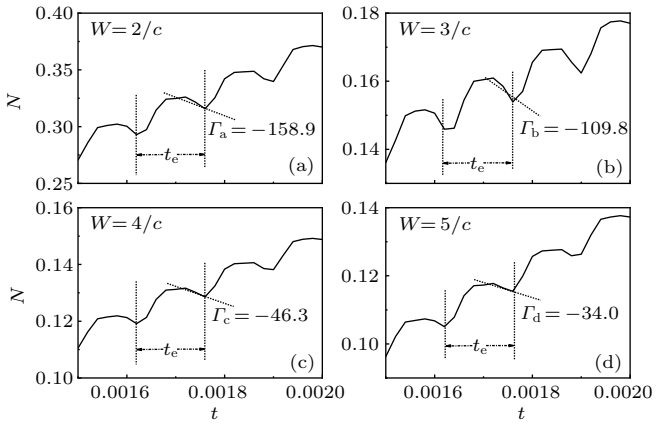


Fig. 3. Time evolution of the total number of the created particles under different widths of the external static electric field. The amplitude and frequency of the oscillating field is $V_1 = c^2$ and $\omega = 2.5c^2$, the intensity of the external static electric field is $V_2 = 0.8c^2$.

4. The spatial density and momentum distribution of the created particles

To observe the annihilation phenomena in space and the effect of the static field on the trajectory of the created particles, here we focus on the spatial density distributions of the created particles under different intensities of the external static field V_2 at $t = 0.002$.

In Fig. 4, the picture show the simulated results of the created electrons, while the positrons moves toward the opposite direction. Here we set same parameters as Fig. 1. The dotted curve is the spatial density while $V_2 = 0$, which is symmetric about $z_0 = -0.3$, because there exist two directions of the initial velocities for the created particles in an one-dimensional model, and the created particles cannot be accelerated or decelerated while the external static field intensity is absent. The created particles will move out from the center of the interaction region with a constant velocity to both sides, thus results in a symmetric distribution. It is worth mentioning that, due to the Pauli exclusion principle, the creation of new particles will be blocked for a fermionic system, and should be promoted if the created particles are pulled out of the interaction region.

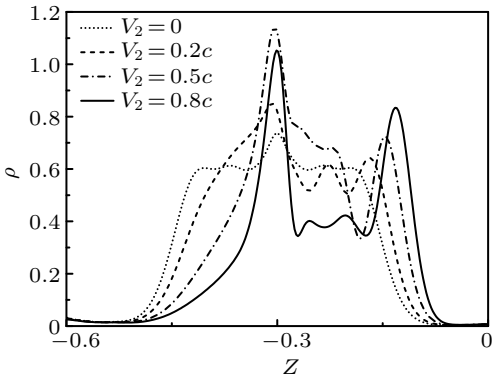


Fig. 4. The spatial density distribution of the created electrons under different intensities of the external static field V_2 at $t = 0.002$. The amplitude and frequency of the oscillating field is $V_1 = c^2$ and $\omega = 2.5c^2$, when the field widths is $W = 3/c$. The center of the fields is located at $z_0 = -0.3$.

It is observed that for the dashed curve, which are simulated with a static field intensity $V_2 = 0.2c^2$, the created particles exists in $-0.3 < z < 0$ and $-0.6 < z < -0.3$ regions at $t = 0.002$. Under such a static field, half the created particles which move to the right direction are accelerated, and other particles which move to the left direction are decelerated. For a static field with intensity $V_2 = 0.2c^2$ that is less than the critical intensity $V_2 = 0.5c^2$ as we estimated in Section 3, due to the asymmetric distribution of the external field, the spatial density distribution is no longer symmetric. In the left region for $-0.6 < z < -0.3$ the created electrons are pushed towards the right direction, compared with that for $V_2 = 0$ (the dotted line), and in the right region for $-0.3 < z < 0$ a small amount of annihilation effect can be observed. This is because, even

for a static field with a weak intensity $V_2 = 0.2c^2$, a small portion of the created particles with slow initial velocities will be dragged back into the interaction region and affect the creation process. For $V_2 = 0.5c^2$ more particles can be dragged back, the curve becomes more asymmetric as presented by the dot-dashed line, and the created electrons are mainly ejected into the region $-0.3 < z < 0$. For an even stronger static field with intensity $V_2 = 0.8c^2$, the created electrons mainly exist in the region $-0.3 < z < 0$, which indicates that most of the created electrons moving toward left are dragged back to the interaction region and annihilate with the antiparticles, and a more obvious annihilation effect can be observed in the right region $-0.3 < z < 0$.

Compare the four different curves, we can find that the created electrons that distribute in the left region for $-0.6 < z < -0.3$ decrease gradually with the increasing intensity of the external static field V_2, and more and more decelerated particles can be dragged back to the interaction region. However, some electrons with high initial kinetic energy still can escape from the interaction region so there also exist a small portion of electrons even for a strong static field with intensity $V_2 = 0.8c^2$. In the right region for $-0.3 < z < 0$, with the increase of the intensity of the static field, the annihilation effect becomes more and more obvious, which is in accordance with the time evolution curve of the total number of the created particles as shown in Fig. 1. It is also worth mentioning that for the electrons that with initial velocities heading toward the right direction, they will be accelerated in the presence of the static field and pushed out of the interaction region directly, thus have no effect on the following creation process.

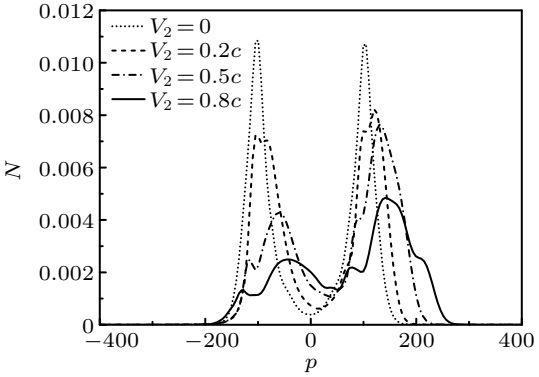


Fig. 5. The momentum distribution of the created electrons under different static field intensities V_2 at $t = 0.002$. The amplitude and frequency of the oscillating field are $V_1 = c^2$ and $\omega = 2.5c^2$ (the same as in Fig. 1).

The momentum distributions give a clearer presentation of the velocities as well as the corresponding energies of the created particles. The simulated results of the created electrons for different intensities of the external static fields are presented in Fig. 5. Here we still set the parameters as $V_1 = c^2$ and $\omega = 2.5c^2$. In Fig. 5, we use different lines to describe the momentum of the created particles under different external static field intensities $V_2 = 0$, $0.2c^2$, $0.5c^2$ and $0.8c^2$, respectively.

Here we also present the results for the created electrons. The dotted line shows the momentum distribution of the created particles without the participation of the static field V_2 at $t = 0.002$. We can observe two symmetric peaks located at $p = \pm 102$, which indicate that the created particles move toward the left and right directions in a one-dimensional model with the same velocity and probability due to the spatial symmetric distribution of the external field. On the other hand, the most probable momentum of the created particles can be estimated according to the relation between the momentum and the total energy, $E^2 = c^2p^2 + c^4$. For a relative wide field as we choose in this paper, the momentum of the system should be conserved, thus resulted in a transition between the energy states $-1.25c^2$ and $1.25c^2$ when the total energy of the created particles is approximately $1.25c^2$ in the simulation parameter $\omega = 2.5c^2$, then the momentum of the created particles should be $p = \pm\sqrt{(E^2 - c^4)/c^2} \simeq \pm 102.8$, which is in accordance with the result shown by the dotted line in Fig. 5.

For other lines in Fig. 5, with the gradually increasing intensity of the static field, the symmetric distribution of the momentum is broken due to the presence of an asymmetric external field. In Fig. 4, the created electrons with positive initial velocity (moving towards the right direction in the region $-0.3 < z < 0$) are accelerated by the static field, while those with negative initial velocity (moving towards the left direction in the region $-0.6 < z < -0.3$) are decelerated. From the perspective of the momentum distribution, a right shift of both peaks can be observed in Fig. 5, while the electrons with positive momentum (indicated by the right peak) gain more momentum for stronger intensity of the static field, and for those with negative momentum (indicated by the left peak) the momentum keeps increasing, even for the opposite signs. For stronger intensities, the corresponding electric field will be stronger and result in larger acceleration, so the right shift will become more obvious, as shown in Fig. 5. As a result, more electrons with the initial negative momentum can be dragged back and head towards the positive direction. We can see that for the dot-dashed line with $V_2 = 0.5c^2$, the probability of the created electrons with positive momentum is much larger than that for the negative momentum, which is in accordance with the result in Fig. 4 for $V_2 = 0.5c^2$, while most of the created electrons distribute in the positive region. Thus, we can consider that, if the intensity of the external static field exceeds the critical value $\omega - 2c^2$, most of the created particles with negative momentum would be dragged back, while the absolute value of the initial velocity of these particles is less than or equal to $\sqrt{2(\omega - 2c^2)}$. Meanwhile, the annihilation effect also becomes more obvious due to the increase of the static field intensity V_2.

In addition, for an external oscillation field with narrower width, the energy of the created particles will be more concentrated. Therefore, for a static field with intensity stronger than the critical value $\omega - 2c^2$, a higher proportion of created electrons can be dragged back and cause more annihilation effect, as pointed out in Fig. 3.

5. Conclusions

In summary, we have discussed the time evolution of the total number of created particles under the combination of a static and an oscillating field. It is found that there are different shapes of the oscillations on these curves with the increasing static field intensity. These oscillations can be considered as an annihilation or creation phenomenon. It is pointed out that the decelerated particles with the initial velocity less than or equal to $c\sqrt{1-4c^4/\omega^2}$ can be dragged back with a static field V_2, which is stronger than the critical value $\omega - 2c^2$, and then annihilate with its antiparticles, thus the total number of created particles is affected. In our simulation, when the frequency of the oscillating field is $\omega = 2.5c^2$, the estimated threshold of the static field should be $V_2 = 0.5c^2$. Therefore, the annihilation phenomenon in the second half cycle $(2n+1)\times t_e/2 < t < (2n+2)\times t_e/2$ can be interpreted to that most of the decelerated particles are dragged back to the interaction region and result in an annihilation effect when $V_2 \geq 0.5c^2$. We also provide the spatial and momentum distribution of the created particles with different intensities of the static field, which confirm the above conclusion.

For an oscillating field with frequency ω that is higher than the energy gap $2c^2$, the particles can be created continuously because of the single-photon transition effect. However, for a fermionic system, due to the Pauli blocking principle, the interaction region is filled with created particles and every state is occupied, the creation rate of the particles will be affected. By adding a static field, the created particles inside the interaction region can be evacuated and therefore increase the total number of created particles. However, for a static field with an intensity that is larger than the critical value $\omega - 2c^2$ as discussed in this paper, other than the particles that are accelerated and pushed out of the interaction region, a large proportion of created particles will be decelerated and dragged back into the interaction region, thus result in an annihilation effect which will cause the decrease of the total number of the created particles.

Although pair creation directly from the vacuum by light can not be achieved under the present experimental condition, many proposals have been raised regarding different combinations of the external electric fields. For a model with a high frequency oscillating field in a static field background, or two overlapping laser beams with substantially different frequencies when one field can be considered to be static, the results in this paper are applicable, and the annihilation effect must be considered.

References

[1] Schwinger J 1951 *Phys. Rev.* **82** 664
[2] Narozhny N B, Bulanov S S, Mur V D and Popov V S 2004 *JETP Lett.* **80** 382
[3] Di Piazza A 2004 *Phys. Rev. D* **70** 053013
[4] Müller C, Hatsagortsyan K Z and Keitel C H 2008 *Phys. Rev. A* **78** 033408
[5] Ruf M, Mocken G R, Müller C, Hatsagortsyan K Z and Keitel C H 2009 *Phys. Rev. Lett.* **102** 080402
[6] Kirk J G, Bell A R and Arka I 2009 *Plasma Phys. Control. Fusion* **51** 085008
[7] Tang S, Xie B S, Lu D, Wang H Y, Fu L B and Liu J 2013 *Phys. Rev. A* **88** 012106
[8] Sang H B, Jiang M and Xie B S 2013 *Chin. Phys. Lett.* **30** 111201
[9] Li Z L, Sang H B and Xie B S 2013 *Chin. Phys. Lett.* **30** 071201
[10] Liu Y, Lv Q Z, Li Y T, Grobe R and Su Q 2015 *Phys. Rev. A* **91** 052123
[11] Piccinelli G and Sánchez A 2017 *Phys. Rev. D* **96** 076014
[12] Li Z L, Xie B S and Li Y J 2019 *Phys. Rev. D* **100** 076018
[13] Krekora P, Su Q and Grobe R 2004 *Phys. Rev. Lett.* **92** 040406
[14] Jiang M, Su W, Lu X, Sheng Z M, Li Y T, Li Y J, Zhang J, Grobe R and Su Q 2011 *Phys. Rev. A* **83** 053402
[15] Wöllert A, Klaiber M, Bauke H and Keitel C H 2015 *Phys. Rev. D* **91** 065022
[16] Schützhold R, Gies H and Dunne G 2008 *Phys. Rev. Lett.* **101** 130404
[17] Monin A and Voloshin M B 2010 *Phys. Rev. D* **81** 085014
[18] Dong S, Unger J, Bryan J, Su Q and Grobe R 2020 *Phys. Rev. E* **101** 013310
[19] Krekora P, Cooley K, Su Q and Grobe R 2005 *Phys. Rev. Lett.* **95** 070403
[20] Jiang M, Lv Q Z, Sheng Z M, Grobe R and Su Q 2013 *Phys. Rev. A* **87** 042503
[21] Lv Q Z, Liu Y, Li Y J, Grobe R and Su Q 2014 *Phys. Rev. A* **90** 013405
[22] Wang Q, Liu J and Fu L b 2016 *Sci. Rep.* **6** 25292
[23] Wang Q, Xia Q Z, Liu J and Fu L B 2018 *Chin. Phys. B* **27** 080302
[24] Su D D, Li Y T, Lv Q Z and Zhang J 2020 *Phys. Rev. D* **101** 054501
[25] Jiang M, Su W, Lv Z Q, Lu X, Li Y J, Grobe R and Su Q 2012 *Phys. Rev. A* **85** 033408
[26] Schneider C and Schützhold R 2016 *J. High Energy Phys.* **2016** 164
[27] Aleksandrov I A, Plunien G and Shabaev V M 2018 *Phys. Rev. D* **97** 116001
[28] Braun J W, Su Q and Grobe R 1999 *Phys. Rev. A* **59** 604
[29] Wagner R E, Ware M R, Shields B T, Su Q and Grobe R 2011 *Phys. Rev. Lett.* **106** 023601
[30] Bandrauk A D and Shen H 1994 *J. Phys. A Math. Gen.* **27** 7147
[31] Mocken G R and Keitel C H 2008 *Comput. Phys. Commun.* **178** 868
[32] Sauter F 1932 *Zeitschrift für Physik* **73** 547
[33] Lin N S, Han L X, Jiang M and Li Y J 2018 *Acta Phys. Sin.* **67** 133401 (in Chinese)